

Reversible Thermosensitive Biodegradable Polymeric Actuators Based on Confined Crystallization

Vladislav Stroganov,^{†,‡} Mahmoud Al-Hussein,[§] Jens-Uwe Sommer,^{†,‡} Andreas Janke,[†] Svetlana Zakharchenko,^{†,‡} and Leonid Ionov^{*,†}

[†]Leibniz-Institut für Polymerforschung Dresden e.V., Hohe Strasse 6, 01069 Dresden, Germany

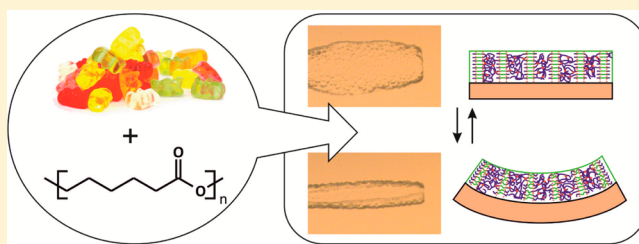
[‡]Technische Universität Dresden, 01062 Dresden, Germany

[§]Department of Physics, The University of Jordan, Amman 11942, Jordan

S Supporting Information

ABSTRACT: We discovered a new and unexpected effect of reversible actuation of ultrathin semicrystalline polymer films. The principle was demonstrated on the example of thin polycaprolactone-gelatin bilayer films. These films are unfolded at room temperature, fold at temperature above polycaprolactone melting point, and unfold again at room temperature. The actuation is based on reversible switching of the structure of the hydrophobic polymer (polycaprolactone) upon melting and crystallization. We hypothesize that the origin of this unexpected behavior is the orientation of polycaprolactone chains parallel to the surface of the film, which is retained even after melting and crystallization of the polymer or the “crystallization memory effect”. In this way, the crystallization generates a directed force, which causes bending of the film. We used this effect for the design of new generation of fully biodegradable thermoresponsive polymeric actuators, which are highly desirable for bionano-technological applications such as reversible encapsulation of cells and design of swimmers.

KEYWORDS: Reversible actuators, thermoresponsive, polycaprolactone, confined crystallization, stimuli-responsive



Polymer actuators are materials capable of changing their shape in response to variation of environmental conditions, thus performing mechanical work. There are many kinds of polymer actuators such as liquid crystals, where actuation is achieved by cooperative reorganization of mesogen groups,¹ hydrogels based on reversible swelling,² shape memory polymers based on temperature-induced relaxation,³ as well as actuators where the driving force is surface tension.⁴ Polymer actuators have been used for many applications such as controlling the liquid flow in microfluidical devices actuators,^{5–9} designing of swimmers,^{10,11} walkers,¹² sensors,^{13,14} imaging devices,^{15,16} and 3D microfabrication.¹⁷ One of the promising fields of applications of polymeric actuators is the design of biomaterials such as stents,¹⁸ sutures,¹⁹ as well as bioscaffolds.^{20–22} For such kind of applications, polymeric actuators must be both biocompatible and biodegradable. Moreover, the set of stimuli, which can be used in living systems, is substantially limited. While UV light harms the cells and can cause DNA damage, changes in pH in a broad range is also not possible. Nonetheless, the cells can survive in a broad temperature range between 4 and 37 °C and therefore the temperature can be used as a signal to trigger actuation.

Examples of biocompatible/biodegradable thermoresponsive polymers with LCST behavior, which can be used for the design of actuators, have been reported in the literature.²³ However, these polymers are sensitive to pH and ionic strength

that strongly affect their switching temperatures. Other examples of temperature-sensitive biodegradable shape memory polymers, which undergo one way transition only have been also demonstrated.²⁴ In contrast, very recently Lendlein reported macroscopic shape memory polymers with reversible actuation.^{25,26} They are based on two cross-linked crystalline polymers with different melting points. The polymer is deformed at a temperature above the melting points of both polymers and then cooled down to room temperature. During cooling, the polymer with the higher melting point crystallizes first and forms a framework/scaffold, which restricts the mobility of the second polymer chains. Heating above the melting point of the polymer with the lower melting point results in partial relaxation of shape of the polymer. Cooling down leads to the recrystallization of this polymer, which is guided by the framework of the first polymer that recovers the deformed shape.

In this paper we report biodegradable thermoresponsive polymeric films with reversible actuation based on polycaprolactone-gelatin bilayers. In a previous work, we demonstrated that this system can be used for one-way folding or one-way folding and unfolding.²⁷ The actuation was based on switching

Received: November 24, 2014

Revised: January 26, 2015

Published: February 4, 2015

of the swelling properties of the gelatin layer. Gelatin swelled in water and caused bending of the bilayer. In contrast, the reversible actuator we demonstrate here is based on switching of the properties of the hydrophobic polymer (PCL) that is guided by confined crystallization of the polymer chains in thin films.

Results and Discussions. We fabricated gelatin-PCL films by sequential dip coating of pure gelatin and PCL containing 4-hydroxybenzophenone. The thickness of gelatin and PCL layers were 1.6 μm and 500 nm, respectively. The film was irradiated by UV light (254 nm) through a photomask to cross-link the polymers. The film was rinsed in organic solvent in order to remove non-cross-linked PCL. The obtained film was exposed to water (Figure 1a). Similar to the previously described

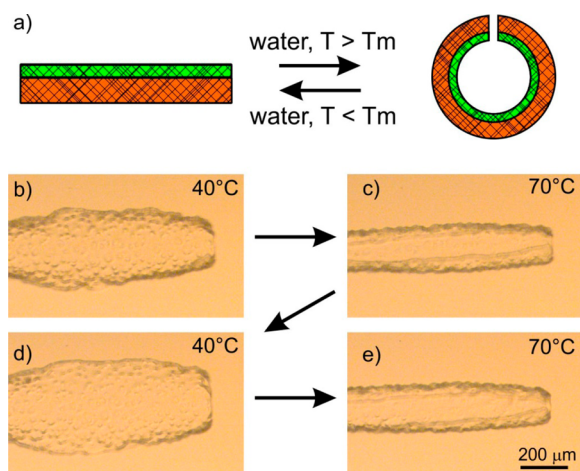


Figure 1. Thermoresponsive actuation of thin gelatin-PCL films (see Video_S1_actuation, Supporting Information); (a) scheme of actuation of (red is gelatin, green is PCL); (b–e) microscopy snapshots of gelatin-PCL bilayer at different temperatures.

approach²⁷ both cross-linked and non-cross-linked gelatin swelled in water. Increase of the temperature led to the dissolution of non-cross-linked gelatin at ~ 40 °C. On the other hand, contrary to the experiments described in our previous paper, dissolution of gelatin did not result in folding of the bilayer film and it remained undeformed at 40 °C (Figure 1b). However, further heating above 60 °C led to the rolling of the films and the formation of tubes (Figure 1c). Subsequent cooling to room temperature led to the recovery of the initial shape (unfolding, Figure 1d). The folding and unfolding was exhibited by the same bilayer film many times upon successive heating–cooling cycles indicating the reversibility of the actuation process (Figure 1e).

In order to explain the observed folding/unfolding, we investigated the responsive properties of the gelatin and PCL layers. Cross-linked gelatin films were swollen up to 1000–1200 vol % in water. The swelling degree was found to be independent of temperature within a range of 20–80 °C. Moreover, repetitive cooling and heating did not influence the swelling degree. The PCL layer demonstrated on the other hand responsive properties. Heating resulted in a volume expansion and a substantial decrease in the elastic modulus. We found that the volume of the PCL layer increased by $\sim 10\%$ upon heating to 65 °C. The change of the elastic modulus was more considerable ($E_{\text{PCL},23\text{ }^\circ\text{C}} = 524 \pm 78$ MPa, $E_{\text{PCL},65\text{ }^\circ\text{C}} = 0.617 \pm 0.032$ MPa). Cooling down to room temperature led

to the recovery of the initial volume and elastic modulus. Therefore, we conclude that heating the bilayer film in the range 20–80 °C results in switching the properties of the PCL layer solely, whereas the gelatin layer remains swollen in the entire temperature range.

We modeled the radius of curvature of the folded bilayer in the states when the PCL layer is hard (low temperatures) and when it is soft (high temperatures) using Timoshenko equation (for details see Supporting Information).²⁸ The results of the modeling are shown in Figure 2. As can be seen, increasing the

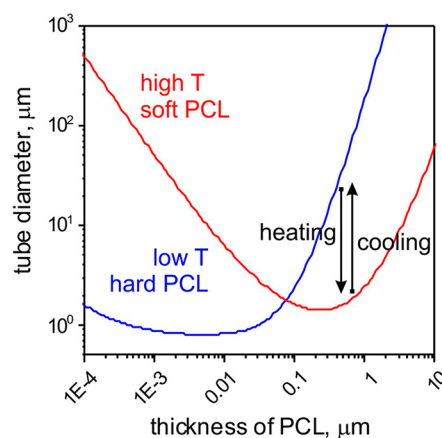


Figure 2. Estimated dependence of diameter of gelatin-PCL tubes on thickness of PCL layer obtained using Timoshenko eq 1; see Supporting Information.

thickness of the PCL layer leads first to a decrease in the radius of curvature. It then reaches a certain minimum value and further increase of the thickness of the PCL layer leads to an increase in the radius of curvature. The position of the curve minimum depends on the elastic modulus of the PCL layer. Decreasing E_{PCL} leads to a shift in the position of the curve minimum to higher values of the thickness of the PCL layer. The left region of the curve corresponds to very thin films. Such bilayer must roll and form tubes at low temperatures. In our experiments, the thickness of the PCL layer is ~ 500 nm, which corresponds to the minimum on the red curve (soft PCL, Figure 2) and upward slope in blue curve (hard PCL). The values predicted by Timoshenko equation appear to be lower in comparison with the experimentally observed diameter of the tube, although it is able to qualitatively explain why the bilayer is undeformed at room temperature and folds when the PCL layer becomes soft at temperatures >60 °C. Indeed, contrary to previous experiments,²⁷ we used thicker PCL layer, which is stiffer and does not allow rolling of the bilayer at room temperature even if the gelatin is swollen.

To elucidate the origin of the unfolding, which occurs upon cooling, we performed a set of experiments. In the first experiment, we found that folded gelatin-PCL bilayers with non-cross-linked PCL folded upon heating but were unable to unfold during subsequent cooling. In the second experiment, the same behavior was found for tubes with 5 μm thick cross-linked PCL layer. They folded upon heating but no unfolding was observed upon cooling. Apparently, in the first case we observe a plastic (irreversible) deformation of the PCL chains that is intrinsic to non-cross-linked polymers. These experiments show that cross-linking and the thickness of the PCL

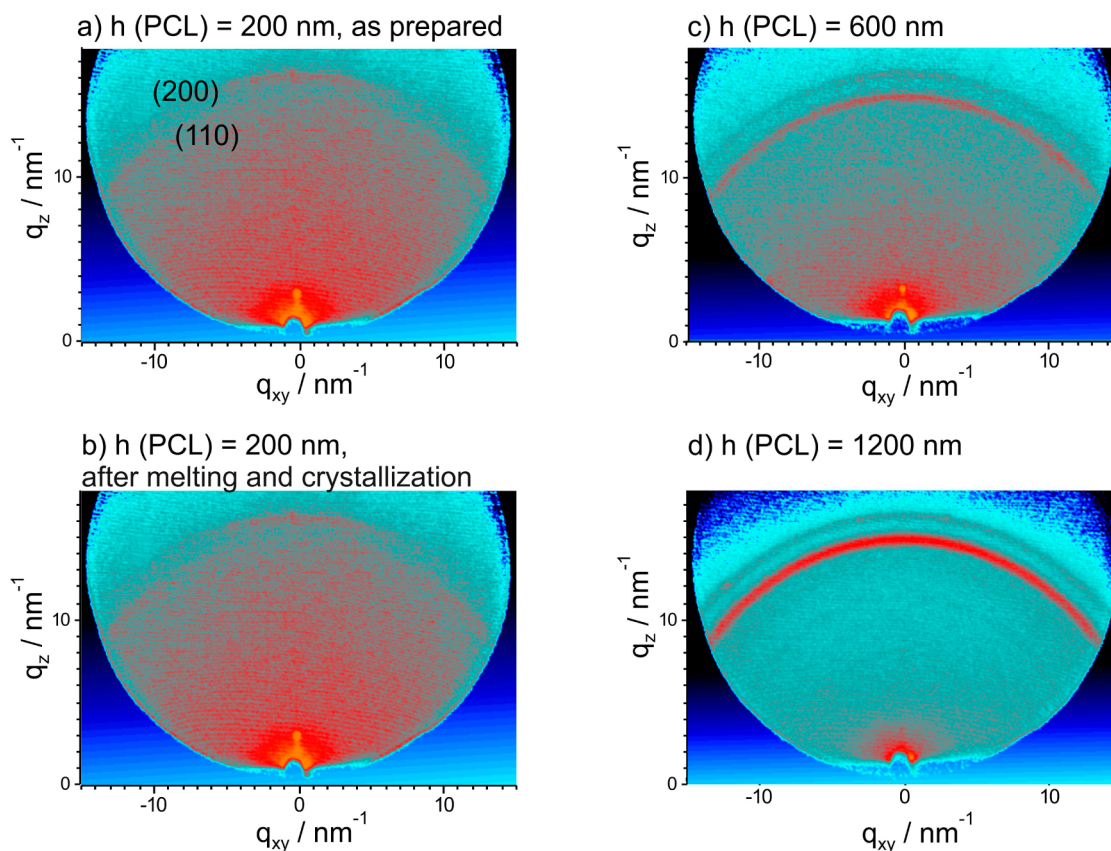


Figure 3. Two-dimensional grazing incidence X-ray scattering patterns of PCL films deposited on gelatin on silicon substrates of thicknesses: (a) 200 nm before melting and (b) after melting and recrystallization of the film of (a); (c) 600 nm, (d) 1200 nm.

layer play a crucial role in attaining reversible folding/unfolding bilayer films.

In order to determine the effect of the thickness of the PCL layer we investigated the morphology and structure of 200 nm, 500 nm, and 5 μm thick PCL layers. All films exhibit spherulites typical of semicrystalline polymers. The size of the spherulites depends on thickness of the PCL layer (Supporting Information Figure S1). Smaller spherulites are observed in the case of 5 μm thick PCL film and very large spherulites are observed in the case of the very thin films because of reduction of number of primary nucleation sites.

The crystalline structure of the PCL films with different thicknesses was investigated using GIWAXS (scattering geometry of the experiment is illustrated in Supporting Information Figure S2). We found that all PCL films are semicrystalline as evidenced by the typical (110) and (200) reflections of the PCL crystals. It is known that PCL crystallizes in an orthorhombic structure with unit cell dimensions: $a = 7.496 \text{ \AA}$, $b = 4.974 \text{ \AA}$, and $c = 17.297 \text{ \AA}$ (chain axis).²⁹ The films with different thicknesses have nearly the same degree of crystallinity $\sim 40\%$ (Supporting Information Figure S3). Temperature-dependent GIWAXS measurements showed that the melting points of the thin films are 3–5° lower than the melting point of the thick film (see Supporting Information, Figure S4). This indicates a poorer crystalline organization in thin films. More importantly, detailed XRD investigation showed a preferential orientation of the chains in the crystalline regions of the PCL layer parallel to the surface in thin films and no preferred orientation in thick films (for details see Supporting Information). The preferential orientation of the

polymer chains is retained after melting of the film and its second crystallization (Figure 3b). In light of these results, we can conclude that the formation of the edge-on lamellae is significantly affected by the PCL film thickness.

In fact, the dependence of lamellae orientation on thin film thickness has already been observed for many semicrystalline polymers, including PCL.^{30–35} However, in contrast to the edge-on orientation of our system for most of these polymers the lamellae were oriented flat-on to the substrate, that is, with the polymer chain axis perpendicular to the substrate. Upon decreasing the film thickness, the crystalline lamellae can have a preferential orientation relative to the substrate influenced by polymer–substrate (gelatin) interactions. In contrast, thicker polycrystalline films tend to have more overlapped crystalline domains leading to bulklike randomly distributed lamellae. We propose that the gelatin layer plays a role in determining the edge-on orientation. The defects on the gelatin layer surface (roughness, dust particle, scratches) serve as nucleation sites that initiate the growth of the crystalline lamellae. However, as the film thickness increases, the gelatin layer effect becomes limited only to adjacent layers of the PCL film and a bulklike behavior dominates in the rest of the film.

In light of these results, we can suggest the following scenario of reversible folding/unfolding of the gelatin-PCL bilayers. The PCL layer is partially crystalline with preferential orientation of chains parallel to the surface of the film (Figure 4a,b). This parallel orientation is caused by confinement effect—small thickness of the PCL film and the influence of the gelatin underlayer. The amorphous phase of the PCL layer is soft ($T_g = -50 \text{ }^\circ\text{C}$) and cross-linked. In contrast, the crystalline phase is

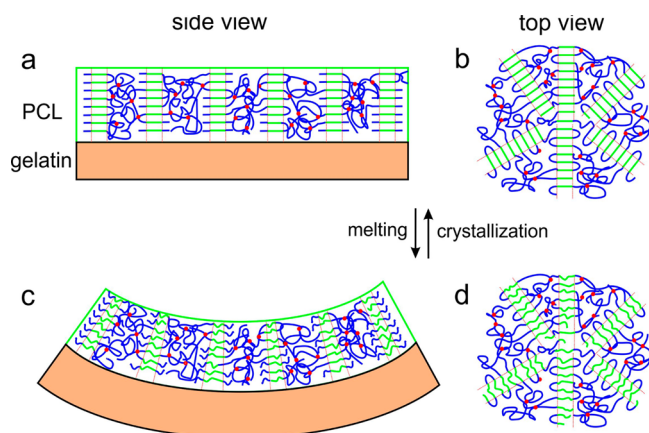


Figure 4. Scheme of reversible actuation of gelatin-PCL films. PCL film consists of amorphous part (blue chains) and crystalline part (green chains). Amorphous part is cross-links (cross-linking points are red). (a,b) Structure of the gelatin-PCL at low temperature (a, side view; b, top view); (b,d) structure of the gelatin-PCL at elevated temperature (c, side view; d, top view).

not cross-linked (cross-linking leads to amorphization of polymer because of the size of photoinitiator molecules) and hard ($T_m = 55\text{--}60\text{ }^\circ\text{C}$). Swelling of the gelatin layer in water generates compressive stresses against the PCL layer. Apparently, the rigid crystalline regions of the PCL layer can withstand such compressive stresses and no bending is observed at room temperature. As demonstrated by the temperature-dependent GIWAXS measurements, heating above $55\text{ }^\circ\text{C}$ leads to the melting of the crystalline phase of the PCL layer making it softer. Because of the substantial loss in the rigidity, the PCL layer can no longer resist the compressive stresses of the gelatin layer causing bending. Since the amorphous part is cross-linked the mobility of polymer chains is substantially restricted. We believe that part of the chains forming the crystalline phase maintain their locations and just undergo transition to disordered state upon melting (Figure 4c,d). Subsequent cooling to room temperature leads to crystallization of the same regions of PCL layer under confinement inducing the chains to assume a parallel orientation to the surface of the film again. The change in conformation of polymer chains generates counter stresses working against the compressive stresses of the gelatin layer. Apparently, recrystallization stresses outweigh the gelatin compressive stresses and the bilayer unfolds upon recrystallization. (Figure 4a,b).

It is worth noting that the mechanism of reversible deformation of PCL-gelatin actuators, which we observed, is different from the mechanisms of reversible deformation described by Lendlein, which involves hard scaffold formed by one of the two polymers.^{25,26} In our case, there is no hard scaffold and the cross-linked amorphous phase of the PCL layer is in a soft rubbery state at room temperature ($T_g = -50\text{ }^\circ\text{C}$). Only this soft part cannot influence the direction of crystallization or its preferential orientation. Therefore, we believe that confinement plays the role of such hard scaffold which guides crystallization. There are other reports of macroscopic two-way shape memory polymers.^{36,37} In one approach,³⁶ the reversibility of actuation is achieved by incomplete melting of polymers. In fact, the part of polymer that is not molten plays a role of rigid scaffold. The part of polymer with low melting point melts and crystallizes during

temperature cycling that leads to change of volume. Irreversible deformation is observed when the polymer is completely melted. We observe reversible actuation even if we go well above melting point of PCL ($T_m(\text{PCL}) = 60\text{ }^\circ\text{C}$), that is, we heat up to more than $70\text{ }^\circ\text{C}$. In another report,³⁷ the cross-linked samples were stretched in molten state to introduce anisotropy, which is required for directed crystallization of polymer chains. In our approach, the anisotropy is generated already during preparation of film by confined crystallization.

In order to estimate the force balance between bending driven by swelling and crystallization (i.e., to estimate if the energy of crystallization is sufficient to cause the deformation of the bilayer), we apply a mean-field approach to the gel-component (the details are given in Supporting Information). If we assume that the shape memory is caused by crystallization of otherwise geometrically blocked parts of the semicrystalline PCL-layer, we should compare the value for energy gain per unit volume (σ) with the free energy gain per volume unit, h , obtained by crystallization. This can be considered as the tension due to crystallization if the film has the freedom to expand against bending to restore the original crystalline domains (Figure 4). Let us estimate the latter by the latent heat of crystallization which is given by $H \cong 142\text{ J/g}$. Given a degree of crystallinity of about 0.5 and the density given by $\rho_{\text{PCL}} \cong 1.2\text{ g/cm}^3$, we obtain $h \cong 8 \times 10^7\text{ Pa}$. From this we can conclude that

$$h \cong 100\sigma$$

In other words, energy gain from crystallization of PCL considerably exceeds the energy gain of swelling of gelatin.

Finally, we demonstrated some applications of the reversibly folding PCL-gelatin thin film. In the first example, we demonstrate a reversible encapsulation and release of bakery yeast cells (Video_S2_Cell_encapsulation, Supporting Information). The cells were adsorbed on the polymer film at room temperature when it was unfolded (Figure 5a). Heating led to

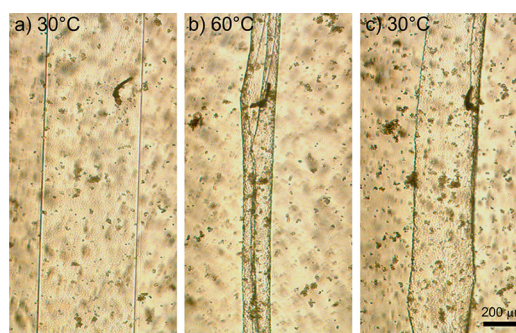


Figure 5. Reversible encapsulation and release of yeast cells inside PCL-gelatin tubes: (a) original state at $30\text{ }^\circ\text{C}$; (b) rolled tube with cells at $60\text{ }^\circ\text{C}$; (c) unrolled bilayer with cells at $30\text{ }^\circ\text{C}$.

rolling of the film and encapsulation of cells inside the tube (Figure 5b). Cooling down unfolded the tube that made the cells accessible (Figure 5c). We also observed that rolling causes movement of the films (Video_S3_actuation, Supporting Information) that can, for example, be used for the design of biodegradable microswimmers.

Conclusions. In this work, we demonstrated and investigated unusual reversible thermoactuation of thin cross-linked polycaprolactone-gelatin films. The films are unfolded at room temperature, fold at temperature above polycaprolactone

melting point, and unfold again at room temperature. We hypothesize that the origin of this unexpected behavior is the orientation of polycaprolactone chains parallel to the surface of the film, which is retained even after melting and crystallization of the polymer. We also demonstrated potential application of such reversible biodegradable thermosensitive actuators for encapsulation of cells. The material that we demonstrated actuates around the melting temperature of polycaprolactone (55–60 °C). We foresee that this temperature can readily be reduced to body temperature, which is more appropriate for experiments with cells, by proper choice of hydrophobic polymer and its composition. We foresee a great potential of the developed approach for cell encapsulation and release, design of scaffolds, and externally controlled microswimmers.

■ ASSOCIATED CONTENT

Supporting Information

Experimental details, details of modeling of bending radius, morphology of PCL films, details of XRD analysis, detailed expiation of mean-field approach as well as videos of actuation of gelatin-PCL films. This material is available free of charge via the Internet at <http://pubs.acs.org>.

■ AUTHOR INFORMATION

Corresponding Author

*E-mail: ionov@ipfdd.de.

Funding

DFG IO68/1–3. M.A.H. thanks The University of Jordan and Leibniz-Institut für Polymerforschung, Dresden (IPF) for financial support.

Notes

The authors declare no competing financial interest.

■ REFERENCES

- (1) Ohm, C.; Brehmer, M.; Zentel, R. *Adv. Mater.* **2010**, *22*, 3366–3387.
- (2) Ionov, L. *Adv. Funct. Mater.* **2013**, *23*, 4555–4570.
- (3) Behl, M.; Razzaq, M. Y.; Lendlein, A. *Adv. Mater.* **2010**, *22*, 3388–3410.
- (4) Azam, A.; Laffin, K. E.; Jamal, M.; Fernandes, R.; Gracias, D. H. *Biomed. Microdevices* **2011**, *13*, 51–58.
- (5) Yu, Q.; Bauer, J. M.; Moore, J. S.; Beebe, D. J. *Appl. Phys. Lett.* **2001**, *78*, 2589–2591.
- (6) Arndt, K.-F.; Kuckling, D.; Richter, A. *Polym. Adv. Technol.* **2000**, *11*, 496–505.
- (7) Dong, L.; Jiang, H. *Soft Matter* **2007**, *3*, 1223–1230.
- (8) Beebe, D. J.; Moore, J. S.; Yu, Q.; Liu, R. H.; Kraft, M. L.; Jo, B.-H.; Devadoss, C. *Proc. Natl. Acad. Sci. U.S.A.* **2000**, *97*, 13488–13493.
- (9) Eddington, D. T.; Beebe, D. J. *Adv. Drug Delivery Rev.* **2004**, *56*, 199–210.
- (10) Kwon, G. H.; Park, J. Y.; Kim, J. Y.; Frisk, M. L.; Beebe, D. J.; Lee, S. H. *Small* **2008**, *4*, 2148–2153.
- (11) Magdanz, V.; Stoychev, G.; Ionov, L.; Sanchez, S.; Schmidt, O. *Angew. Chem., Int. Ed.* **2014**, *126*, 2711–2715.
- (12) Osada, Y.; Okuzaki, H.; Hori, H. *Nature* **1992**, *355*, 242–244.
- (13) Bashir, R.; Hilt, J. Z.; Elibol, O.; Gupta, A.; Peppas, N. A. *Appl. Phys. Lett.* **2002**, *81*, 3091–3093.
- (14) Hilt, J. Z.; Gupta, A. K.; Bashir, R.; Peppas, N. A. *Biomed. Microdevices* **2003**, *5*, 177–184.
- (15) Dong, L.; Agarwal, A. K.; Beebe, D. J.; Jiang, H. *Nature* **2006**, *442*, 551.
- (16) Richter, A.; Paschew, G. *Adv. Mater.* **2009**, *21*, 979–983.
- (17) Ionov, L. *Soft Matter* **2011**, *7*, 6786–6791.
- (18) Yakacki, C. M.; Shandas, R.; Lanning, C.; Rech, B.; Eckstein, A.; Gall, K. *Biomaterials* **2007**, *28*, 2255–2263.
- (19) Lendlein, A.; Langer, R. *Science* **2002**, *296*, 1673–1676.
- (20) Zakharchenko, S.; Pureskiy, N.; Stoychev, G.; Waurisch, C.; Hickey, S. G.; Eychmuller, A.; Sommer, J.-U.; Ionov, L. *J. Mater. Chem. B* **2013**, *1*, 1786–1793.
- (21) Zakharchenko, S.; Sperling, E.; Ionov, L. *Biomacromolecules* **2011**, *12*, 2211–2215.
- (22) Jamal, M.; Kadam, S. S.; Xiao, R.; Jivan, F.; Onn, T.-M.; Fernandes, R.; Nguyen, T. D.; Gracias, D. H. *Adv. Healthcare Mater.* **2013**, *2*, 1142–1150.
- (23) Seuring, J.; Agarwal, S. *ACS Macro Lett.* **2013**, *2*, 597–600.
- (24) Lendlein, A.; Schmidt, A. M.; Langer, R. *Proc. Natl. Acad. Sci. U.S.A.* **2001**, *98*, 842–847.
- (25) Behl, M.; Kratz, K.; Zotzmann, J.; Nochel, U.; Lendlein, A. *Adv. Mater.* **2013**, *25*, 4466–9.
- (26) Behl, M.; Kratz, K.; Nochel, U.; Sauter, T.; Lendlein, A. *Proc. Natl. Acad. Sci. U.S.A.* **2013**, *110*, 12555–12559.
- (27) Stroganov, V.; Zakharchenko, S.; Sperling, E.; Meyer, A. K.; Schmidt, O. G.; Ionov, L. *Adv. Funct. Mater.* **2014**, *24*, 4357–4363.
- (28) Timoshenko, S. *J. Opt. Soc. Am.* **1925**, *11*, 233–255.
- (29) Bittiger, H.; Marchessault, R. H.; Niegisch, W. D. *Acta Crystallogr., Sect. B: Struct. Crystallogr. Cryst. Chem.* **1970**, *26*, 1923–1927.
- (30) Taguchi, K.; Miyaji, H.; Izumi, K.; Hoshino, A.; Miyamoto, Y.; Kokawa, R. *Polymer* **2001**, *42*, 7443–7447.
- (31) Grozev, N.; Botiz, I.; Reiter, G. *Eur. Phys. J. E* **2008**, *27*, 63–71.
- (32) Reiter, G.; Sommer, J.-U. *J. Chem. Phys.* **2000**, *112*, 4376–4383.
- (33) Zhou, W.; Cheng, S. Z. D.; Putthananat, S.; Eby, R. K.; Reneker, D. H.; Lotz, B.; Magonov, S.; Hsieh, E. T.; Geerts, R. G.; Palackal, S. J.; Hawley, G. R.; Welch, M. B. *Macromolecules* **2000**, *33*, 6861–6868.
- (34) Taguchi, K.; Miyamoto, Y.; Miyaji, H.; Izumi, K. *Macromolecules* **2003**, *36*, 5208–5213.
- (35) Sutton, S. J.; Izumi, K.; Miyaji, H.; Miyamoto, Y.; Miyashita, S. *J. Mater. Sci.* **1997**, *32*, 5621–5627.
- (36) Zhou, J.; Turner, S. A.; Brosnan, S. M.; Li, Q.; Carrillo, J.-M. Y.; Nykypanchuk, D.; Gang, O.; Ashby, V. S.; Dobrynin, A. V.; Sheiko, S. *Macromolecules* **2014**, *47*, 1768–1776.
- (37) Chung, T.; Romo-Uribe, A.; Mather, P. T. *Macromolecules* **2007**, *41*, 184–192.